Measurements and Simulations of Ultralow Emittance and Ultrashort Electron Beams in the Linac Coherent Light Source

Y. Ding, A. Brachmann, F.-J. Decker, D. Dowell, P. Emma, J. Frisch, S. Gilevich, G. Hays, Ph. Hering, Z. Huang, R. Iverson, H. Loos, A. Miahnahri, H.-D. Nuhn, D. Ratner, J. Turner, J. Welch, W. White, and J. Wu

SLAC National Accelerator Laboratory, 2575 Sand Hill Road, Menlo Park, California 94025, USA

(Received 30 January 2009; published 24 June 2009)

The Linac Coherent Light Source (LCLS) is an x-ray free-electron laser project presently in a commissioning phase at the SLAC National Accelerator Laboratory. We report here on very low-emittance measurements made at low bunch charge, and a few femtosecond bunch length produced by the LCLS bunch compressors. Start-to-end simulations associated with these beam parameters show the possibilities of generating hundreds of GW at 1.5 Å x-ray wavelength and nearly a single longitudinally coherent spike at 1.5 nm with 2-fs duration.

DOI: 10.1103/PhysRevLett.102.254801 PACS numbers: 41.60.Cr, 29.25.Bx, 29.27.Bd

Free-electron lasers (FELs) hold great promise as tunable, high-power, coherent sources for short-wavelength radiation. Several x-ray FEL projects are being developed worldwide as next-generation light sources [1–3]. A key requirement in realizing x-ray FELs is a high-brightness electron beam that possesses high peak current and very low transverse emittance. The design of these advanced light sources typically assumes a bunch charge of ~ 1 nC in order to reach sufficient peak current to drive an x-ray FEL. However, due to the strong interaction of the bunch self-field throughout the accelerator, creating and preserving a low-emittance bunch at such a high charge is a tremendous challenge. In this Letter, we experimentally demonstrate the generation of ultra-low-emittance and ultrashort electron beams when operating the Linac Coherent Light Source (LCLS) injector and accelerator in a low-charge mode. Although the bunch charge used in these experiments ($\sim$20 pC) is much lower than the standard case of 1 nC, the final bunch length is compressed to ~ 1 μm by magnetic bunch compression, resulting in an ultrashort bunch with beam brightness higher than the conventional design at 1 nC charge. Simulations suggest such a bunch is capable of generating intense x rays in the LCLS undulator with a few femtosecond pulse duration and hence may open up new parameter regimes for the LCLS and other x-ray FEL projects under consideration. Similar low-charge operating schemes for high gain FELs have also been suggested before [4,5], and efforts are under way at the Paul Scherrer Institute to develop an ultra-low-emittance source at low bunch charge [6].

The LCLS injector [7] and main linac [8] have been fully commissioned and have already produced an electron beam with adequate brightness to drive the x-ray FEL. The high-brightness electron beam will be transported into the FEL undulator starting in early 2009. During the 2008 commissioning phase, the electron bunch was fully characterized at several different operating points, including a high charge mode (1 nC), a more routine setting (0.25 nC), and also a very low charge level (0.02 nC). Although the machine operates well at 0.25 nC with a transverse normalized emittance of <1 μm, there is also growing interest in a much lower bunch charge, where femtosecond pulses may be possible and injector emittance levels down to 0.14 μm have recently been observed at LCLS (see Table I).

The injector emittance measurements are made using an intercepting 1-μm thick aluminum screen (''OTR2'' in Fig. 1) after acceleration to 135 MeV, where the transverse electron beam size is measured using optical transition radiation (OTR) to image the spot onto a digital camera. The field of an upstream quadrupole focusing magnet is varied over several settings while the horizontal beam size is measured on the OTR screen, following the common ''quad-scan'' method of analyzing the transverse emittance. In addition, an *S*-band (2856 MHz) rf deflector cavity upstream of the screen (see ''TCAV0'' in Fig. 1) is used to streak the beam vertically across the screen in order to time-resolve the horizontal emittance. The horizontal

TABLE I. Measured (@ 20-pC and 250-pC) and design (@ 1-nC) LCLS parameters.

Parameter[a]	20 pC	250 pC	1 nC	Unit
UV laser energy on cathode	1.5	20	250	μJ
UV spot diameter on cathode	0.6	1.2	2	mm
UV pulse duration (fwhm)	4.0	6.5	10	ps
Injector bunch length (rms)	1.3	2.5	2.8	ps
Initial peak current	5	30	100	A
Injector slice emittance	0.14	0.6	1.0	μm
Injector projected emittance	0.20	0.7	1.2	μm
Final bunch length (rms)	$\sim$3	$\sim$30	80	fs
Final peak current	$\sim$3	$\sim$3	3.4	kA
Final projected emittance	0.4	1.0	1.5	μm
FEL pulse duration (fwhm)[b]	$\sim$2	$\sim$60	230	fs
FEL peak power[b]	$\sim$400	$\sim$20	$\sim$10	GW

[a]Emittance refers to normalized emittance; fwhm stands for full width half maximum; rms stands for root mean square.
[b]Based on simulations at 1.5 Å wavelength.

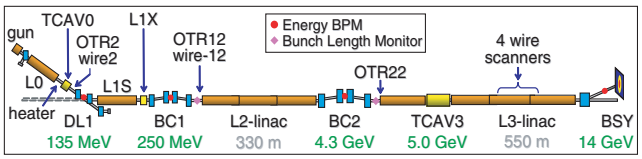

FIG. 1 (color online). LCLS 1-km accelerator layout showing gun, off-axis injector, BC1 and BC2 compressors, and various linac segments. The undulator (not shown) is 400 m off scale at right.

emittance is then sliced up 15 bins in time and plotted versus the bunch length time coordinate in Fig. 2. The emittance error bars are derived from the scatter of the beam size measurements during the ''quad scan,'' with 10 beam pulses at each quadrupole strength. The central slice of this ''time-sliced'' emittance is then measured at a constant 20-pC bunch charge as a function of the rms UV laser spot size on the cathode (1/4 of its diameter for a uniform distribution) and plotted in Fig. 3 with red (or gray) points.

The thermal emittance is taken from the core time-sliced emittance measurements at 20 pC as a function of laser spot size, assuming space charge forces and external field aberrations can be ignored. The space charge contribution is minimized by measuring at low charge and also by time slicing the emittance. Figure 3 summarizes the thermal emittance characteristics of the copper cathode in the LCLS gun. The measured thermal emittance is given as the slope of the data (0.91 μm/mm) and a theoretical slope (see below) is also shown.

The normalized thermal emittance for photoemission from a metal can be shown to be [9]

$$\gamma\epsilon_{\text{thermal}} = \sigma_x\sqrt{\frac{\hbar\omega - \phi_{\text{eff}}}{3mc^2}}, \qquad (1)$$

where σ_x is the transverse rms laser beam size on the cathode, $\hbar\omega$ is the UV laser photon energy (4.90 eV), ϕ_{eff} is the effective work function of the metal, and mc^2 is the electron rest mass energy. With a measured quantum efficiency of 6×10^{-5} the effective work function is 4.52 eV. Equation (1) then gives an expected thermal emittance of 0.50 μm/mm, as shown in Fig. 3. This is approximately half the level of the measured thermal emittance, which may be due to cathode nonuniformity as well as a small contribution from space charge. This result is consistent with previous measurements using rf guns performed at the Brookhaven National Laboratory [10]. It is interesting to note that recent measurements made with a dc gun [11] are in much better agreement with Eq. (1). Work is in progress to understand these differences.

The low-charge electron bunch of 20 pC has also been accelerated in the SLAC linac to 13.6 GeV and compressed in length through the BC1 and BC2 magnetic chicanes. The emittance is measured at an energy of about 10 GeV in the last 200 m of the linac using four wire scanners (see Fig. 1). Each 20-μm diameter tungsten wire is stepped through the electron beam over 20–30 pulses at a bunch repetition rate of 30 Hz and a downstream ion chamber records the intercepted beam signal as a function of wire position in order to reconstruct the averaged transverse beam profile at each of the four wire scanners. The ''time-projected'' emittance is then calculated based on the four measured beam sizes using the known electron optics between scanners. The emittance is then measured at each setting of the L2-linac rf phase, as shown in Fig. 4, which varies the energy chirp along the electron bunch and thus varies the final bunch length after the BC2 compressor chicane.

At nearly the same time, the signal from a photodiode, with bandwidth 1.0–2.5 μm, is measured at each L2-linac rf phase setting. The photodiode is illuminated by the coherent optical transition radiation (COTR) of another OTR screen located just downstream of BC2 (see ''OTR22'' in Fig. 1), where the extremely short bunch passes through the OTR foil radiating coherently at wavelengths longer than the bunch length. The photodiode

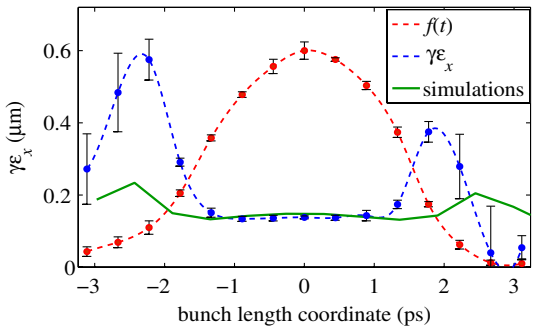

FIG. 2 (color online). Measured (blue or dark gray dots) and simulated (green or gray curve) time-sliced horizontal emittance along the length of the bunch at a charge of 20 pC and cathode UV spot diameter of 0.6 mm. Smooth curves aid the eye and $f(t)$ is the bunch temporal distribution on an arbitrary scale.

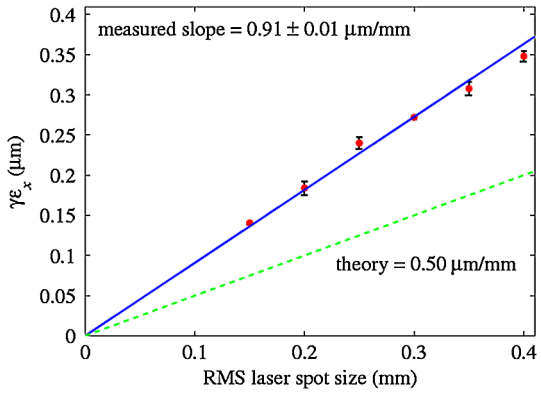

FIG. 3 (color online). Measured core time-sliced emittance at 135 MeV versus rms UV laser spot size (diameter/4) on the cathode with a constant bunch charge of 20 pC (red points). The data are fitted to a single parameter: a linear slope with no offset (blue, solid line). The theoretical thermal emittance is shown in green (dashed) line.

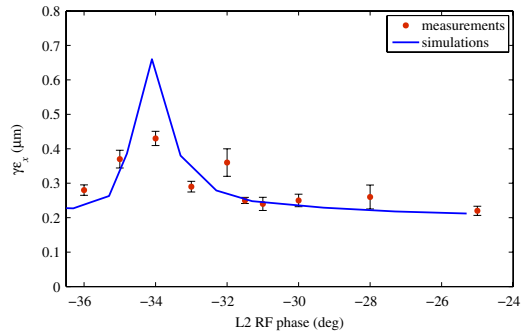

FIG. 4 (color online). Measured (red dots) and simulated (blue curve) projected emittance at 10 GeV versus L2-linac rf phase with a bunch charge of 20 pC.

signal is plotted in Fig. 5 with red (or gray) dots as a function of the L2-linac rf phase indicating that the bunch is compressed to its minimum length at −34.5° (maximum acceleration at crest phase of zero).

Start-to-end computer simulations were carried out from the photocathode to the entrance of the undulator using IMPACT-T [12] and ELEGANT [13] with 1×10^6 macroparticles. IMPACT-T tracks the particles from the photocathode to "OTR2," including 3D space charge force. The initial distribution is based on the measured laser shape, which was longitudinally Gaussian and transversely uniform in these low-charge conditions (Table I). A thermal emittance of 0.14 μm is adopted according to the measurements. The simulated slice emittance at OTR2 agrees well with the measurements as shown in Fig. 2, especially in the core part of the bunch.

The output particles from IMPACT-T are smoothed in the longitudinal phase space to reduce high-frequency numerical noise for subsequent ELEGANT simulations. These particles are then tracked through DL1, linacs, BC1, BC2, and the linac-to-undulator transport beam line to the entrance of the undulator. ELEGANT simulations include linear and nonlinear transport effects, a 1D transient model of CSR, and longitudinal space charge effects, as well as geometric and resistive wake fields in the accelerator. The horizontal emittances from simulations at 10 GeV are shown in Fig. 4

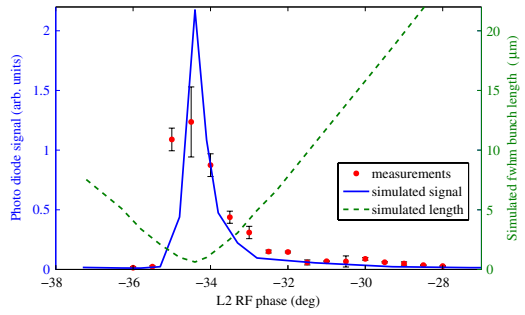

FIG. 5 (color online). Measured (red dots) and simulated (blue curve) photodiode OTR signals at OTR22, versus the L2-linac rf phase with a bunch charge of 20 pC. The green dashed curve (right axis) shows the simulated fwhm bunch length.

with blue (or dark gray) curve, with an rf phase shift of −1.3° to fit the experimental data. This phase shift may come from rf drift during the few hour measurement session, where feedback loops are not operable at the very low charge setting. A particle truncation of 6% was applied to the bunch tails to obtain projected emittance values in simulation which are comparable to measurement methods. These simulations confirm that the transverse emittance is reasonably well preserved, even near maximum bunch compression. This mild emittance growth at full compression is quite different from the sharp emittance growth observed at 250 pC charge [14], presumably due to the much lower charge.

Since the compressed bunch length is not directly measurable at a 1-μm level, we compare the photodiode signal with the integrated bunch form factor over the detector wavelength range (1 to 2.5 μm) from the simulated particle distribution at OTR22. The simulation results are scaled vertically to fit the detector signal (see Fig. 5 in blue or dark gray curve). The same phase shift of −1.3° is also applied to the simulation results. As shown in Fig. 6, when the bunch is undercompressed (phase $>$ − 34.5°), the current distribution shows sharp spikes at bunch head and tail. When the bunch is overcompressed (phase $<$ − 34.5°), the head-tail spikes disappear, forming a more Gaussian bunch, and the coherent signal drops sharply. These different temporal shapes lead to the asymmetry of the photodiode signal in Fig. 5. The reasonable agreement between measurements and simulations for these OTR signals show that the minimum bunch length may be below 1 μm for this very low-charge scenario, as shown from the simulated bunch length (green or gray dashed curve) in Fig. 5.

The macroparticles dumped from ELEGANT are used as an input for the GENESIS 1.3 [15] FEL code to evaluate the FEL performance. The longitudinal wake field in the undulator is negligible at this low charge and is not included in these simulations. In order to generate very short x-ray

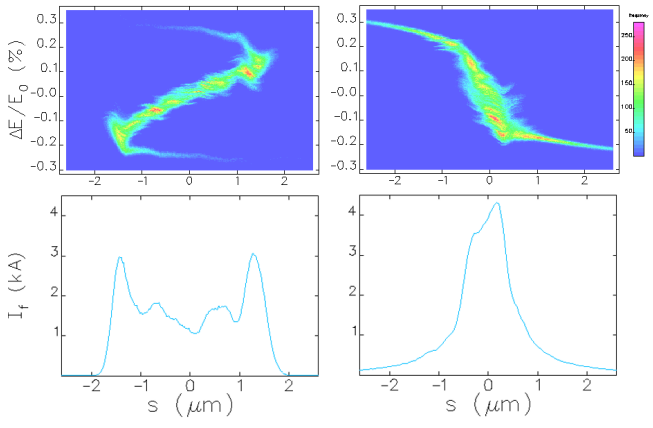

FIG. 6 (color online). Longitudinal phase space at OTR22 after undercompression (top left) and overcompression (top right), and the corresponding current profiles below. The L2 rf phases for the two compression modes are at −33.5° and −35°. The bunch head is to the left.

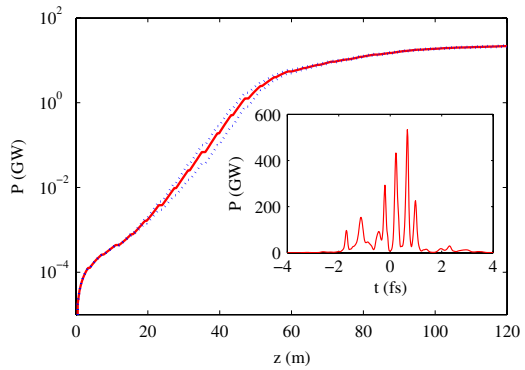

FIG. 7 (color online). GENESIS simulation at 1.5 Å for the average FEL power (solid line) and the rms fluctuation (dashed lines) along the undulator. The inset plot shows a snapshot of a typical 2-fs FEL pulse at 100 m.

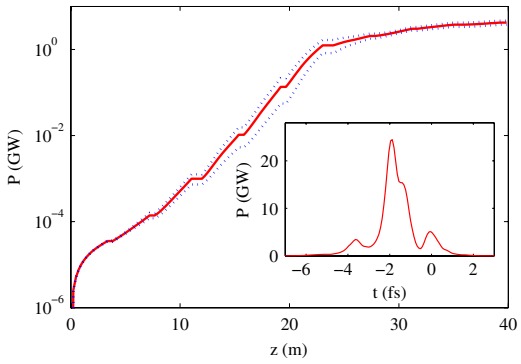

FIG. 8 (color online). GENESIS simulation at 15 Å for the average FEL power (solid line) and the rms fluctuation (dashed lines) along the undulator. The inset plot shows a snapshot of a typical 2-fs FEL pulse at 25 m (inset).

pulses, it is advantageous to operate BC2 in the over-compression mode where the current is higher in the central part of the bunch instead of the double-horn current profile from an under-compressed bunch. This can be achieved when operating L2-linac at $-35°$ (hereafter the phase represents the experimental phase, which is $-1.3°$ shifted from simulations). At this phase, ELEGANT tracking shows that a peak current above 3 kA can be expected at the undulator entrance. As shown in Fig. 7, the simulated x-ray power at 1.5 Å saturates at about 60 m of undulator length, well within the LCLS total undulator length (132 m). The inset plot also shows a typical FEL power profile near the end of the LCLS undulator approaching 500 GW with a fwhm x-ray pulse duration of about 2 fs. The integrated photon flux is about 3×10^{11} for this 2-fs x-ray pulse with 3% statistical fluctuation due to shot noise startup. The x-ray pulse length can be varied by adjusting L2-linac rf phase to change the compression ratio on the electron bunch after passing BC2.

When the LCLS is operated at a beam energy of 4.3 GeV (turning off L3-linac), soft x-ray photons of 800 eV (1.5 nm in wavelength) will be produced. Because of this longer radiation wavelength and hence stronger slippage effect in the undulator, a single x-ray spike with full longitudinal coherence may be expected. In the over-compression mode, with the L2-linac phase setting at $-35.5°$, the GENESIS simulation in Fig. 8 shows the 1.5 nm FEL may reach saturation at $z = 25$ m with nearly a single longitudinal spike of 2 fs duration. The integrated photon flux is about 2.4×10^{11} with 20% statistical fluctuation at this saturation point.

In summary, we have shown the extraordinary brightness of a low-charge bunch produced by the LCLS injector and accelerator. FEL simulations indicate such a bunch may generate hundreds of GW of hard x-ray power at 1.5 Å and nearly a single longitudinal spike of 2 fs at 1.5-nm wavelength. Such high-power, ultrashort x-ray pulses may open up new applications in many areas of science. In addition, the achieved beam brightness may enable a more compact design of a future hard x-ray FEL facility, where a much lower-energy linac than the LCLS and a shorter-period undulator can be envisioned to drive a hard x-ray FEL.

We thank the SLAC engineering, controls, operations, and rf support groups for their help and dedicated support, and we also thank R. Fiorito, C. Pellegrini, G. Stupakov, and D. Xiang for helpful discussions. This work was supported by Department of Energy Contract No. DE-AC02-76SF00515.

[1] LCLS Conceptual Design Report, SLAC-R-593, 2002.
[2] TESLA Technical Design Report, TESLA FEL 2002-09, 2002.
[3] SPring-8 Compact SASE Source Conceptual Design Report, http://www-xfel.spring8.or.jp (2005).
[4] J. Rosenzweig *et al.*, Nucl. Instrum. Methods Phys. Res., Sect. A **593**, 39 (2008).
[5] X. J. Wang *et al.*, Nucl. Instrum. Methods Phys. Res., Sect. A **507**, 310 (2003).
[6] R. Ganter *et al.*, Phys. Rev. Lett. **100**, 064801 (2008).
[7] R. Akre *et al.*, Phys. Rev. ST Accel. Beams **11**, 030703 (2008).
[8] R. Akre *et al.*, in *Proceedings of the FEL2008 Conference*, http://accelconf.web.cern.ch/accelconf/index.html.
[9] D. H. Dowell and J. Schmerge, Report No. SLAC-PUB-13535.
[10] W. Graves *et al.*, in *Proceedings of the PAC01 Conference*, http://accelconf.web.cern.ch/accelconf/index.html, pp. 2227–2229.
[11] Y. Kim *et al.*, in Proceedings of the FEL2008 Conference (Ref. [8]).
[12] J. Qiang *et al.*, Phys. Rev. ST Accel. Beams **9**, 044204 (2006).
[13] M. Borland, ELEGANT, Advanced Photon Source LS-287, 2000.
[14] K. Bane *et al.*, Phys. Rev. ST Accel. Beams **12**, 030704 (2009).
[15] S. Reiche *et al.*, Nucl. Instrum. Methods Phys. Res., Sect. A **429**, 243 (1999).